

# Introduction to cell-centered Lagrangian schemes

**François Vilar**

Institut Montpellierain Alexander Grothendieck  
Université de Montpellier

September 13th, 2017



**IMAG**  
INSTITUT MONTPELLIERAIN  
ALEXANDER GROTHENDIECK



- 1 Introduction
- 2 Gas dynamics system of equations
- 3 First-order numerical scheme for the 2D gas dynamics
- 4 High-order extension in the 2D case
- 5 Numerical results in 2D

## Eulerian formalism (spatial description)

- fixed referential attached to the observer
- fixed observation zone through the fluid flows

## Lagrangian formalism (material description)

- moving referential attached to the material
- observation zone moved and deformed as the fluid flows

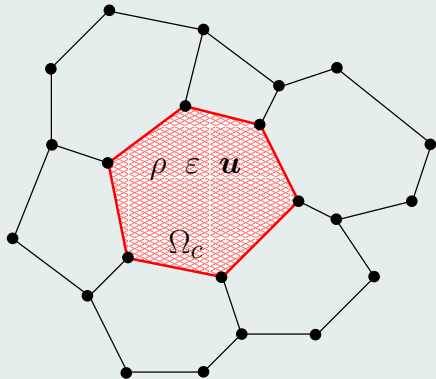
## Lagrangian formalism advantages

- adapted to problems undergoing large deformations
- naturally tracks interfaces in multi-material flows
- avoids the numerical diffusion of the convection terms

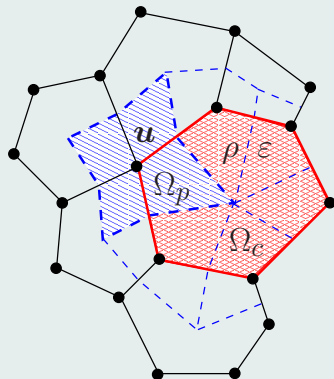
## Lagrangian formalism drawbacks

- **Robustness issue in the case of strong vorticity or shear flows**  
⇒ ALE method (Arbitrary Lagrangian-Eulerian)

## Cell-centered formulation



## Staggered formulation



- 1 Introduction
- 2 Gas dynamics system of equations**
- 3 First-order numerical scheme for the 2D gas dynamics
- 4 High-order extension in the 2D case
- 5 Numerical results in 2D

## Definitions

- $\rho$  the fluid density
- $\mathbf{u}$  the fluid velocity
- $e$  the fluid specific total energy
- $p$  the fluid pressure
- $\varepsilon = e - \frac{1}{2}\mathbf{u}^2$  the fluid specific internal energy

## Euler equations

- $\frac{\partial \rho}{\partial t} + \nabla_x \cdot \rho \mathbf{u} = 0$
- $\frac{\partial \rho \mathbf{u}}{\partial t} + \nabla_x \cdot (\rho \mathbf{u} \otimes \mathbf{u} + p \mathbf{I}_d) = \mathbf{0}$
- $\frac{\partial \rho e}{\partial t} + \nabla_x \cdot (\rho \mathbf{u} e + p \mathbf{u}) = 0$

## Thermodynamical closure

- $p = p(\rho, \varepsilon)$

Equation of state

## Moving referential

- $\mathbf{X}$  is the position of a point of the fluid in its initial configuration
- $\mathbf{x}(\mathbf{X}, t)$  is the actual position of this point, moved by the fluid flow

## Trajectory equation

- $\frac{\partial \mathbf{x}(\mathbf{X}, t)}{\partial t} = \mathbf{u}(\mathbf{x}(\mathbf{X}, t), t)$
- $\mathbf{x}(\mathbf{X}, 0) = \mathbf{X}$

## Material derivative

- $f(\mathbf{x}, t)$  is a smooth fluid variable
- $\frac{d f(\mathbf{x}, t)}{d t} = \frac{\partial f(\mathbf{x}, t)}{\partial t} + \mathbf{u} \cdot \nabla_{\mathbf{x}} f(\mathbf{x}, t)$

## Definitions

- $\tau = \frac{1}{\rho}$  the specific volume
- $\mathbf{U} = (\tau, \mathbf{u}, \mathbf{e})^t$  the solution vector
- $\mathbf{F}(\mathbf{U}) = (-\mathbf{u}, \mathbb{1}(1)\rho, \mathbb{1}(2)\rho, \mathbb{1}(3)\rho, \rho\mathbf{u})^t$  where  $\mathbb{1}(i) = (\delta_{i1}, \delta_{i2}, \delta_{i3})^t$
- $a = a(\rho, \varepsilon)$  the sound speed

## Updated Lagrangian formulation

- $\rho \frac{d\mathbf{U}}{dt} + \nabla_x \cdot \mathbf{F}(\mathbf{U}) = 0$

Moving configuration

## Non-conservative formulation

- $\rho \frac{d\mathbf{U}}{dt} + \mathbf{A}_x(\mathbf{U}) \frac{\partial \mathbf{U}}{\partial x} + \mathbf{A}_y(\mathbf{U}) \frac{\partial \mathbf{U}}{\partial y} + \mathbf{A}_z(\mathbf{U}) \frac{\partial \mathbf{U}}{\partial z} = 0$
- $\mathbf{A}_n = \mathbf{A}_x n_x + \mathbf{A}_y n_y + \mathbf{A}_z n_z$  with  $\mathbf{n}$  a unit vector
- $\lambda(\mathbf{U}) = \{-\rho a, 0, \rho a\}$  the eigenvalues of  $\mathbf{A}_n(\mathbf{U})$



## Deformation gradient tensor

- $\mathbf{J} = \nabla_{\mathbf{x}} \mathbf{x}$
- $|\mathbf{J}| = \det \mathbf{J} > 0$
- $\nabla_{\mathbf{x}} \cdot (|\mathbf{J}| \mathbf{J}^{-t}) = \mathbf{0}$

Jacobian of the fluid flow

Positive control volume

Piola compatibility condition

## Mass conservation

- $\int_{\omega(0)} \rho^0 dV = \int_{\omega(t)} \rho dV$
- $\int_{\omega(t)} \rho dV = \int_{\omega(0)} \rho |\mathbf{J}| dV$
- $\rho |\mathbf{J}| = \rho^0$

## Total Lagrangian formulation

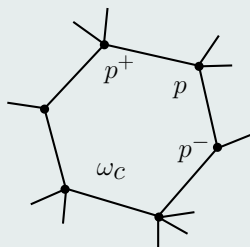
- $\rho^0 \frac{d\mathbf{U}}{dt} + \nabla_{\mathbf{x}} \cdot (|\mathbf{J}| \mathbf{J}^{-1} \mathbf{F}(\mathbf{U})) = \mathbf{0}$

Fixed configuration

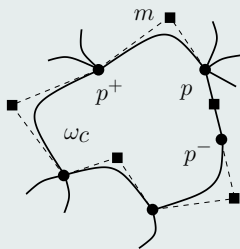
- 1 Introduction
- 2 Gas dynamics system of equations
- 3 First-order numerical scheme for the 2D gas dynamics**
- 4 High-order extension in the 2D case
- 5 Numerical results in 2D

## Définitions

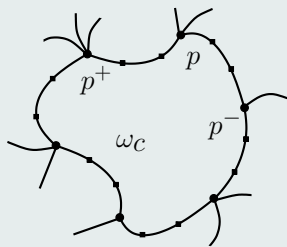
- $0 = t^0 < t^1 < \dots < t^N = T$  a partition of the time domain  $[0, T]$
- $\omega^0 = \bigcup_{c=1,l} \omega_c^0$  a partition of the initial domain  $\omega^0$
- $\omega_c^n$  the image of  $\omega_c^0$  at time  $t^n$  through the fluid flow
- $m_c$  the constant mass of cell  $\omega_c$
- $U_c^n = (\tau_c^n, u_c^n, e_c^n)^t$  the discrete solution



(a) Straight line edges



(b) Conical edges



(c) Polynomial edges

Figure: Generic polygonal cell

## Integration

- $$U_c^{n+1} = U_c^n - \frac{\Delta t^n}{m_c} \int_{\partial\omega_c} \bar{\mathbf{F}} \cdot \mathbf{n} ds$$
- Integration of the cell boundary term (analytically, quadrature, ...)

## General first-order finite volumes scheme

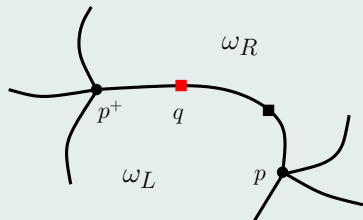
- $$U_c^{n+1} = U_c^n - \frac{\Delta t^n}{m_c} \sum_{q \in \mathcal{Q}_c} \bar{\mathbf{F}}_{qc} \cdot l_{qc} \mathbf{n}_{qc}$$
- $\bar{\mathbf{F}}_{qc} = (-\bar{\mathbf{u}}_q, \mathbb{1}(1)\bar{p}_{qc}, \mathbb{1}(2)\bar{p}_{qc}, \bar{p}_{qc} \bar{\mathbf{u}}_q)^t$  numerical flux at point  $q$
- $\mathbf{x}_q^{n+1} = \mathbf{x}_q^n + \Delta t^n \bar{\mathbf{u}}_q$

## Definitions

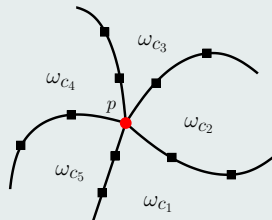
- $\mathcal{Q}_c$  the chosen control point set of cell  $\omega_c$
- $l_{qc} \mathbf{n}_{qc}$  some normals to be defined

## Remark

- $\bar{F}_{qc}$  is local to the cell  $\omega_c$
- Only  $\bar{\mathbf{u}}_{qc} = \bar{\mathbf{u}}_q$  needs to be continuous, to advect the mesh
- Loss of the scheme conservation?



(a) Face control point



(b) Grid node

Figure: Points neighboring cell sets

## 1D numerical fluxes

- $\bar{p}_{qc} = p_c^n - \tilde{z}_{qc} (\bar{\mathbf{u}}_q - \mathbf{u}_c^n) \cdot \mathbf{n}_{qc}$
- $\tilde{z}_{qc} > 0$  local approximation of the acoustic impedance

## Conservation

- $\sum_c m_c \mathbf{U}_c^{n+1} = \sum_c m_c \mathbf{U}_c^n + \text{BC} \quad ?$
- For sake of simplicity, we consider  $\text{BC} = 0$
- Necessary condition:  $\sum_c \sum_{q \in \mathcal{Q}_c} \bar{\rho}_{qc} l_{qc} \mathbf{n}_{qc} = \mathbf{0}$

## Example of a solver: LCCDG schemes

- Conditions suffisantes
- $\forall p \in \mathcal{P}(\omega), \quad \sum_{c \in \mathcal{C}_p} [\bar{\rho}_{pc}^- l_{pc}^- \mathbf{n}_{pc}^- + \bar{\rho}_{pc}^+ l_{pc}^+ \mathbf{n}_{pc}^+] = \mathbf{0}$ 

$$\implies \bar{\mathbf{u}}_p = \left( \sum_{c \in \mathcal{C}_p} M_{pc} \right)^{-1} \sum_{c \in \mathcal{C}_p} \left( M_{pc} \mathbf{u}_c^n + \rho_c^n l_{pc} \mathbf{n}_{pc} \right)$$
- $\forall q \in \mathcal{Q}(\omega) \setminus \mathcal{P}(\omega), \quad (\bar{\rho}_{qL} - \bar{\rho}_{qR}) l_{qL} \mathbf{n}_{qL} = \mathbf{0} \iff \bar{\rho}_{qL} = \bar{\rho}_{qR}$ 

$$\implies \bar{\mathbf{u}}_q = \left( \frac{\tilde{Z}_{qL} \mathbf{u}_L^n + \tilde{Z}_{qR} \mathbf{u}_R^n}{\tilde{Z}_{qL} + \tilde{Z}_{qR}} \right) - \frac{\rho_R^n - \rho_L^n}{\tilde{Z}_{qL} + \tilde{Z}_{qR}} \mathbf{n}_{qf_{pp^+}}$$

## Convex combinaison

- $$U_c^{n+1} = U_c^n - \frac{\Delta t^n}{m_c} \sum_{q \in Q_c} \bar{F}_{qc} \cdot l_{qc} \mathbf{n}_{qc} + \frac{\Delta t^n}{m_c} F(U_c^n) \cdot \underbrace{\sum_{q \in Q_c} l_{qc} \mathbf{n}_{qc}}_{=0}$$
- $$U_c^{n+1} = (1 - \lambda_c) U_c^n + \sum_{q \in Q_c} \lambda_{qc} \bar{U}_{qc}$$

## Definitions

- $$\lambda_{qc} = \frac{\Delta t^n}{m_c} \tilde{z}_{qc} l_{qc} \quad \text{and} \quad \lambda_c = \sum_{q \in Q_c} \lambda_{qc}$$
- $$\bar{U}_{qc} = U_c^n - \frac{(\bar{F}_{qc} - F(U_c^n))}{\tilde{z}_{qc}} \cdot \mathbf{n}_{qc}$$

## CFL condition

- $$\Delta t^n \leq \frac{m_c}{\sum_{q \in Q_c} \tilde{z}_{qc} l_{qc}} \left( = \frac{|\omega_c^n|}{a_c^n \sum_{q \in Q_c} l_{qc}} \quad \text{if} \quad \tilde{z}_{qc} \equiv z_c^n = \rho_c^n a_c^n \right)$$

## Semi-discret first-order scheme

- $$m_c \frac{dU_c}{dt} = - \sum_{q \in Q_c} \bar{F}_{qc} \cdot l_{qc} \mathbf{n}_{qc}$$

## Gibbs identity

- $$T dS = d\varepsilon + p d\tau = d\mathbf{e} - \mathbf{u} \cdot d\mathbf{u} + p d\tau$$

## Semi-discret production of entropy

- $$m_c T_c \frac{dS_c}{dt} = m_c \frac{d\mathbf{e}_c}{dt} + \mathbf{u}_c \cdot m_c \frac{d\mathbf{u}_c}{dt} + p_c m_c \frac{d\tau_c}{dt}$$
- $$m_c T_c \frac{dS_c}{dt} = \sum_{q \in Q_c} \tilde{z}_{qc} l_{qc} [(\bar{\mathbf{u}}_q - \mathbf{u}_c) \cdot \mathbf{n}_{qc}]^2 \geq 0$$

## Positivity of the discrete scheme



F. VILAR, C.-W. SHU AND P.-H. MAIRE, *Positivity-preserving cell-centered Lagrangian schemes for multi-material compressible flows: Form first-order to high-orders. Part II: The 2D case.* JCP, 2016.



- 1 Introduction
- 2 Gas dynamics system of equations
- 3 First-order numerical scheme for the 2D gas dynamics
- 4 High-order extension in the 2D case**
- 5 Numerical results in 2D

## High-order extension of the finite-volume scheme

- MUSCL, (W)ENO, DG, ...

## Mean values equation

- $$U_c^{n+1} = U_c^n - \frac{\Delta t^n}{m_c} \sum_{q \in Q_c} \bar{F}_{qc} \cdot l_{qc} \mathbf{n}_{qc}$$
- In  $\bar{F}_{qc}$ , the mean values are substituted by the high-order values  $U_{qc}$  in  $\omega_c$  at points  $q$

## Updated or total Lagrangian formulation

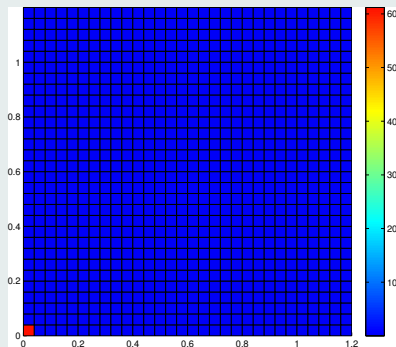
- $$\rho \frac{dU}{dt} + \nabla_x \cdot F(U) = 0 \quad \text{ou} \quad \rho^0 \frac{dU}{dt} + \nabla_x \cdot (|J|J^{-1}F(U)) = 0$$

## Piecewise polynomial approximation

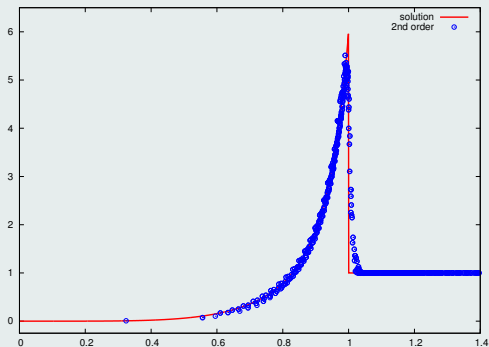
- $U_{h,c}^n(\mathbf{x})$  the polynomial approximation of the solution on  $\omega_c^n$
- $U_{h,c}^n(\mathbf{X})$  the polynomial approximation of the solution on  $\omega_c^0$
- $U_{qc} = U_{h,c}^n(\mathbf{x}_q)$  (moving config.) or  $U_{qc} = U_{h,c}^n(\mathbf{X}_q)$  (fixed config.)

- 1 Introduction
- 2 Gas dynamics system of equations
- 3 First-order numerical scheme for the 2D gas dynamics
- 4 High-order extension in the 2D case
- 5 Numerical results in 2D**

# Sedov point blast problem



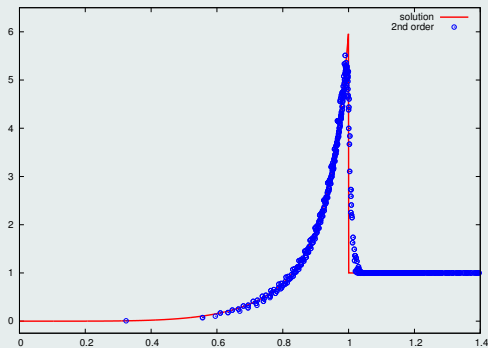
(a) Pressure field



(b) Density profiles

Figure : Solution at time  $t = 1$  for a Sedov problem on a  $30 \times 30$  Cartesian mesh

# Sedov point blast problem

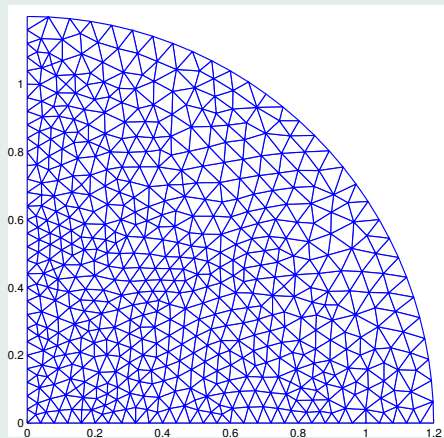


(a) Pressure field

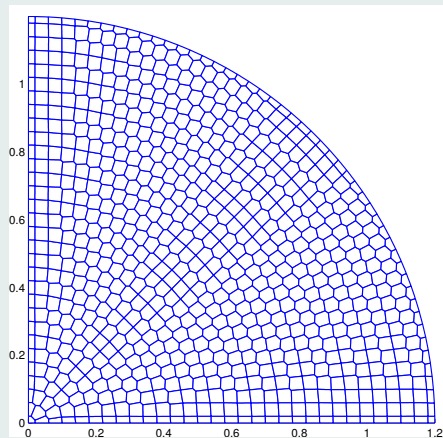
(b) Density profiles

Figure : Solution at time  $t = 1$  for a Sedov problem on a  $30 \times 30$  Cartesian mesh

# Sedov point blast problem



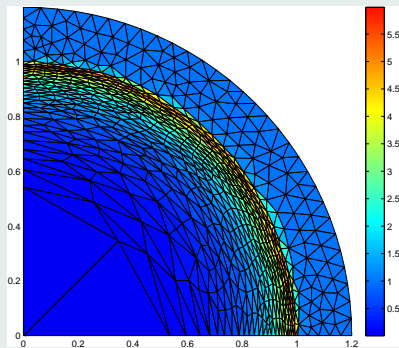
(c) Triangular grid - 1110 cells



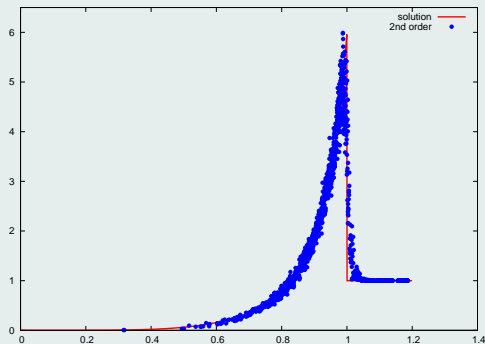
(d) Polygonal grid - 775 cells

**Figure** : Initial unstructured grids for Sedov point blast problem

# Sedov point blast problem



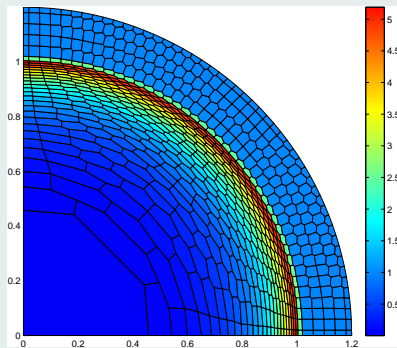
(e) Density field



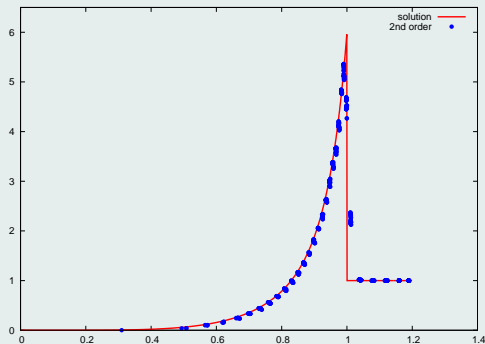
(f) Density profiles

**Figure :** Solution at time  $t = 1$  for a Sedov problem on a grid made of 1110 triangular cells

# Sedov point blast problem



(g) Density field

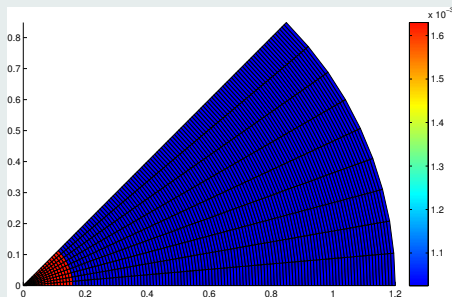


(h) Density profiles

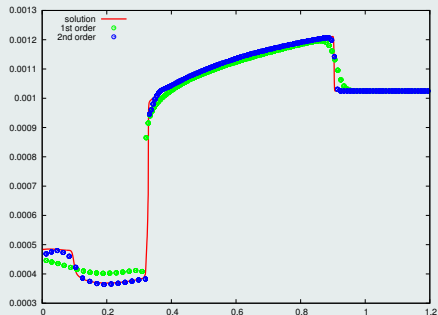
**Figure :** Solution at time  $t = 1$  for a Sedov problem on a grid made of 775 polygonal cells



# Underwater TNT explosion



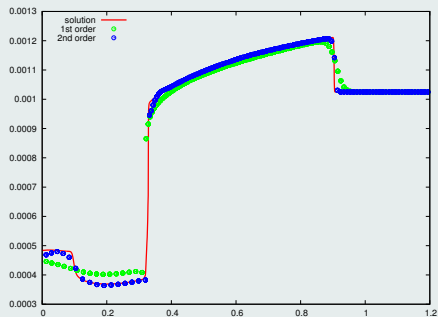
(i) Density field - 2nd order



(j) Density profiles

**Figure :** Solution at time  $t = 2.5 \times 10^{-4}$  for a underwater TNT explosion on a  $120 \times 9$  polar mesh

# Underwater TNT explosion



(i) Density field - 2nd order

(j) Density profiles

**Figure :** Solution at time  $t = 2.5 \times 10^{-4}$  for a underwater TNT explosion on a  $120 \times 9$  polar mesh

## Aluminium projectile impact problem

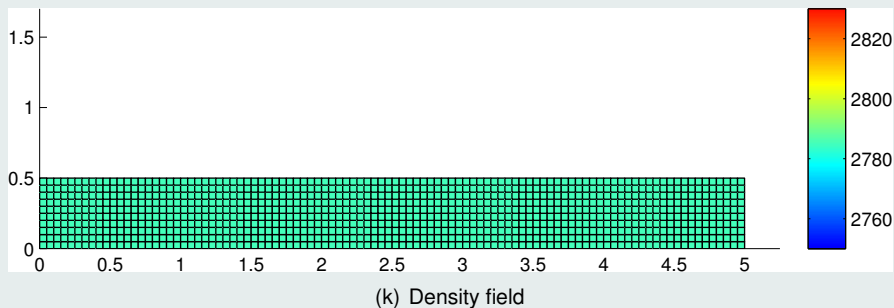


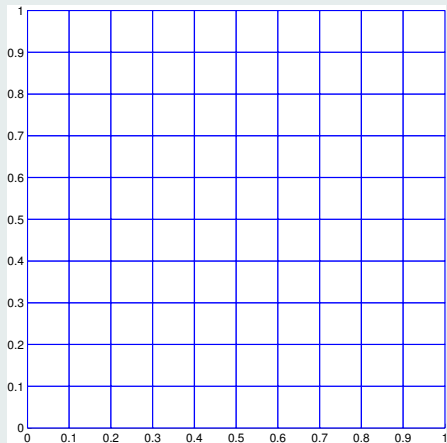
Figure : Solution at time  $t = 0.05$  for a projectile impact problem on a  $100 \times 10$  Cartesian mesh

## Aluminium projectile impact problem

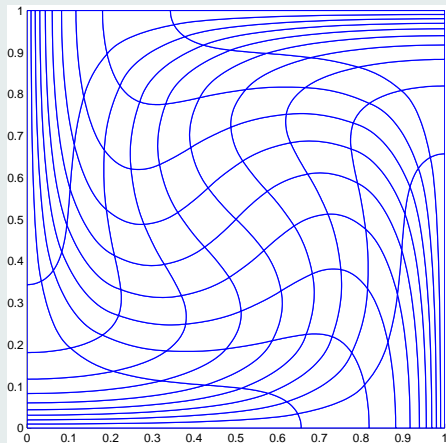
(k) Density field

**Figure :** Solution at time  $t = 0.05$  for a projectile impact problem on a  $100 \times 10$  Cartesian mesh

# Taylor-Green vortex



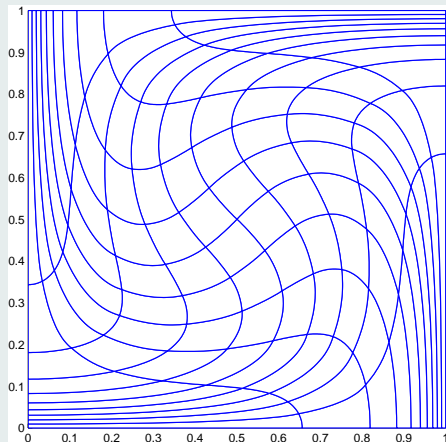
(l) 2nd order



(m) Exact solution

Figure : Final deformed grids at time  $t = 0.75$ , on a  $10 \times 10$  Cartesian mesh

# Taylor-Green vortex



(l) 2nd order

(m) Exact solution

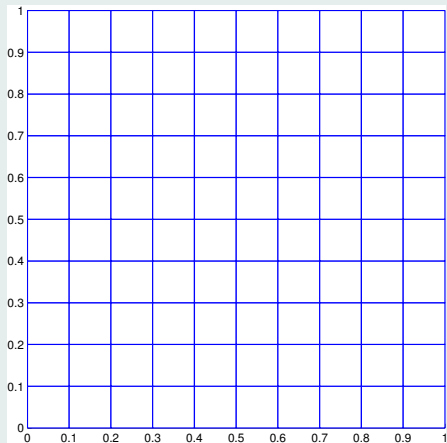
Figure : Final deformed grids at time  $t = 0.75$ , on a  $10 \times 10$  Cartesian mesh

## Convergence rates

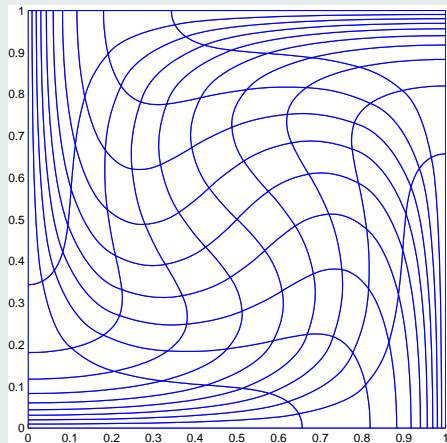
	$L_1$		$L_2$		$L_\infty$	
$h$	$E_{L_1}^h$	$q_{L_1}^h$	$E_{L_2}^h$	$q_{L_2}^h$	$E_{L_\infty}^h$	$q_{L_\infty}^h$
$\frac{1}{10}$	5.06E-3	1.94	6.16E-3	1.93	2.20E-2	1.84
$\frac{1}{20}$	1.32E-3	1.98	1.62E-3	1.97	5.91E-3	1.95
$\frac{1}{40}$	3.33E-4	1.99	4.12E-4	1.99	1.53E-3	1.98
$\frac{1}{80}$	8.35E-5	2.00	1.04E-4	2.00	3.86E-4	1.99
$\frac{1}{160}$	2.09E-5	-	2.60E-5	-	9.69E-5	-

**Table:** Convergence rates on the pressure for a 2nd order DG scheme

# Taylor-Green vortex



(n) 3rd order



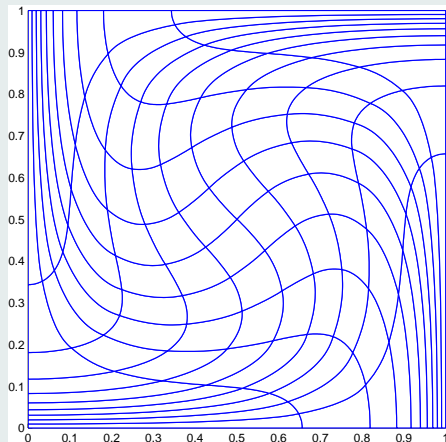
(o) Exact solution

Figure : Final deformed grids at time  $t = 0.75$ , on a  $10 \times 10$  Cartesian mesh



# Taylor-Green vortex

(n) 3rd order



(o) Exact solution

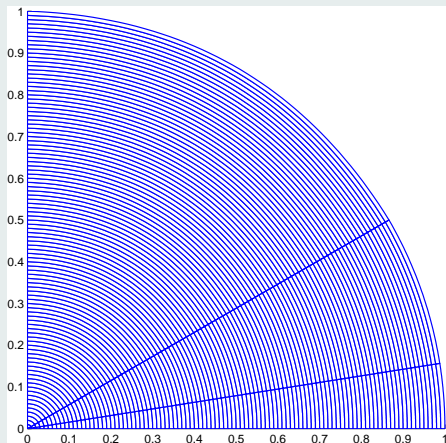
Figure : Final deformed grids at time  $t = 0.75$ , on a  $10 \times 10$  Cartesian mesh

## Convergence rates

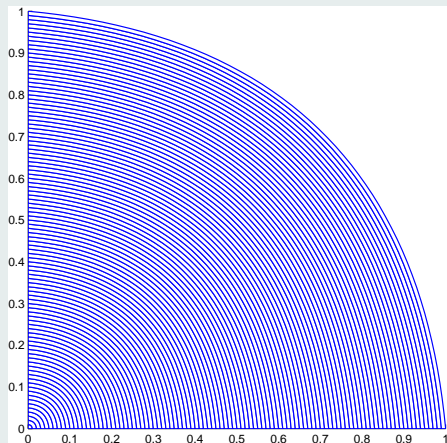
	$L_1$		$L_2$		$L_\infty$	
$h$	$E_{L_1}^h$	$q_{L_1}^h$	$E_{L_2}^h$	$q_{L_2}^h$	$E_{L_\infty}^h$	$q_{L_\infty}^h$
$\frac{1}{10}$	2.67E-4	2.96	3.36E-7	2.94	1.21E-3	2.86
$\frac{1}{20}$	3.43E-5	2.97	4.36E-5	2.96	1.66E-4	2.93
$\frac{1}{40}$	4.37E-6	2.99	5.59E-6	2.98	2.18E-5	2.96
$\frac{1}{80}$	5.50E-7	2.99	7.06E-7	2.99	2.80E-6	2.99
$\frac{1}{160}$	6.91E-8	-	8.87E-8	-	3.53E-7	-

**Table:** Convergence rates on the pressure for a 3rd order DG scheme

## Polar meshes - symmetry preservation



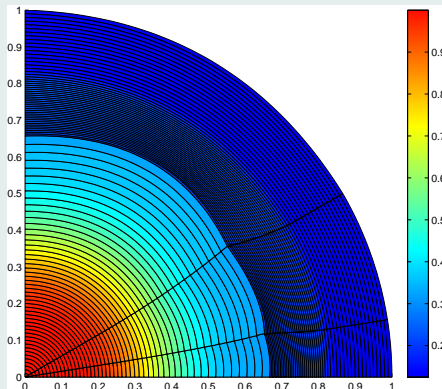
(p)  $100 \times 3$



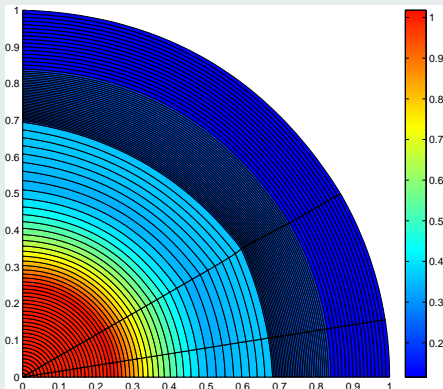
(q)  $100 \times 1$

Figure : Curvilinear grids defined in polar coordinates

# Sod shock tube problem - symmetry preservation



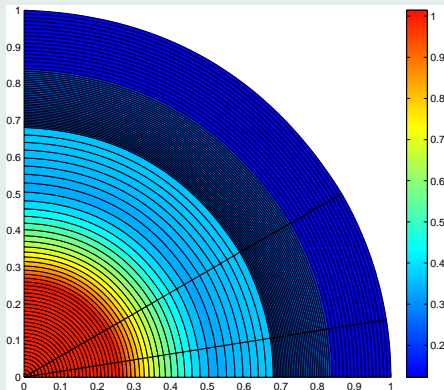
(r) 1st order



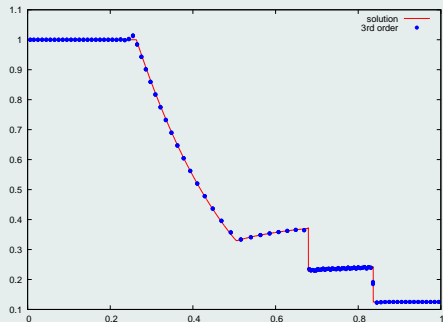
(s) 2nd order

Figure : Density fields with 1st and 2nd order schemes on a 3rd mesh

# Sod shock tube problem - symmetry preservation



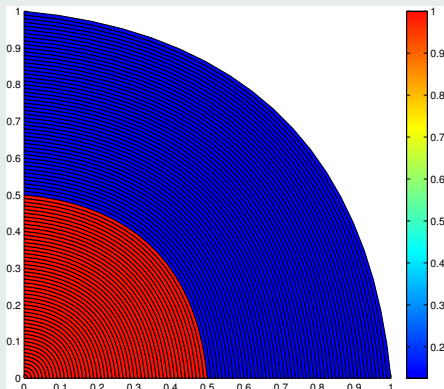
(t) Density field



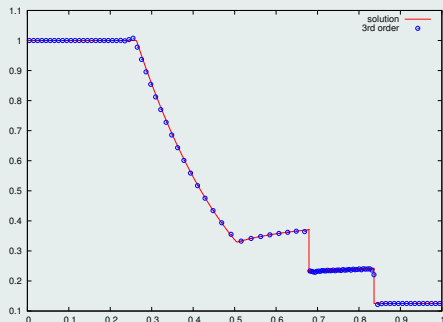
(u) Density profiles

**Figure :** 3rd order solution for a Sod shock tube problem on a  $100 \times 3$  polar grid

# Sod shock tube problem - symmetry preservation



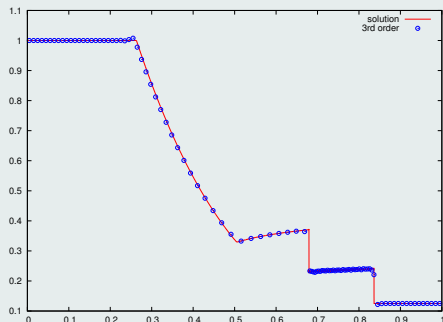
(v) Density field



(w) Density profiles

**Figure :** 3rd order solution for a Sod shock tube problem on a  $100 \times 1$  polar grid

# Sod shock tube problem - symmetry preservation

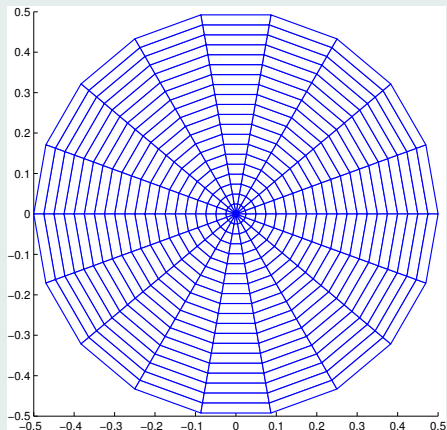


(v) Density field

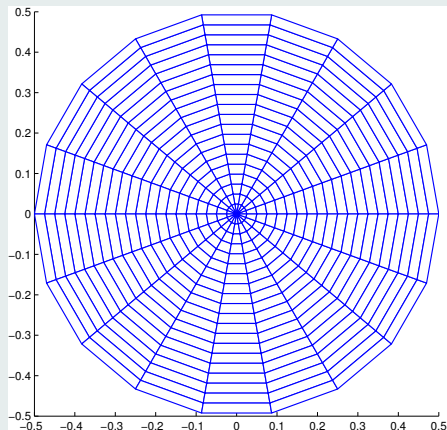
(w) Density profiles

**Figure :** 3rd order solution for a Sod shock tube problem on a  $100 \times 1$  polar grid

# Gresho-like vortex problem



(a) 1st order



(b) 2nd order

Figure : Final deformed grids at time  $t = 1$ , on a  $20 \times 18$  polar mesh



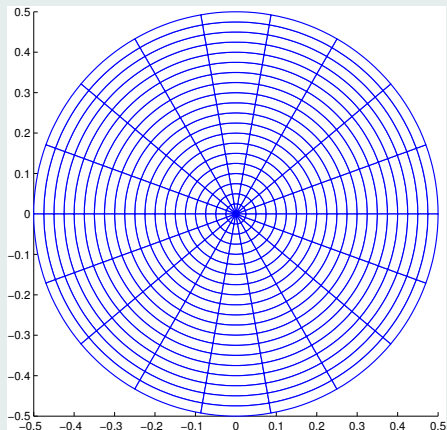
## Gresho-like vortex problem

(a) 1st order

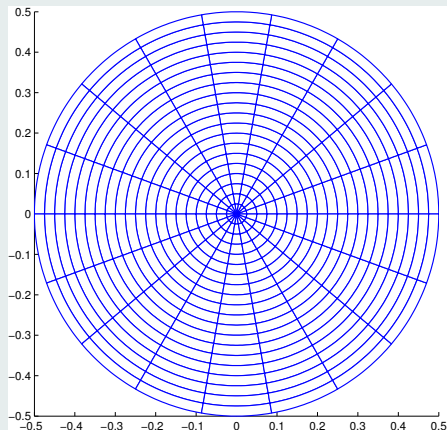
(b) 2nd order

**Figure :** Final deformed grids at time  $t = 1$ , on a  $20 \times 18$  polar mesh

# Gresho-like vortex problem



(c) 3rd order



(d) Exact solution

Figure : Final deformed grids at time  $t = 1$ , on a  $20 \times 18$  polar mesh

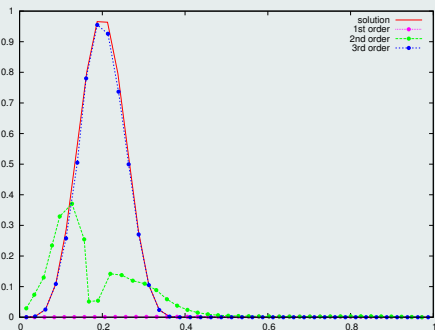
## Gresho-like vortex problem

(c) 3rd order

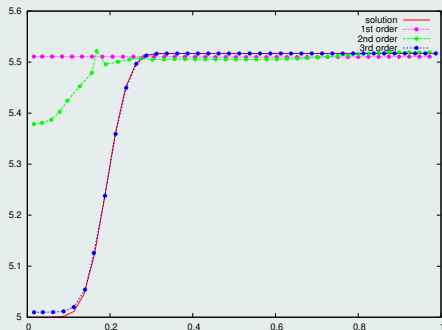
(d) Exact solution

**Figure :** Final deformed grids at time  $t = 1$ , on a  $20 \times 18$  polar mesh

# Gresho-like vortex problem



(e) Velocity profiles



(f) Pressure profiles

**Figure :** Velocity and pressure profiles at time  $t = 1$ , on a  $20 \times 18$  polar grid

# Gresho-like vortex problem

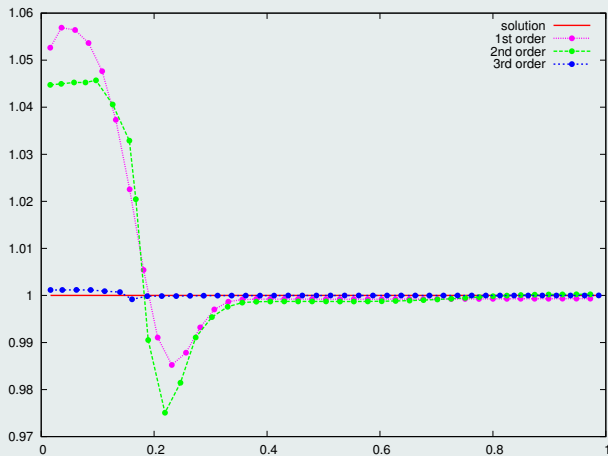
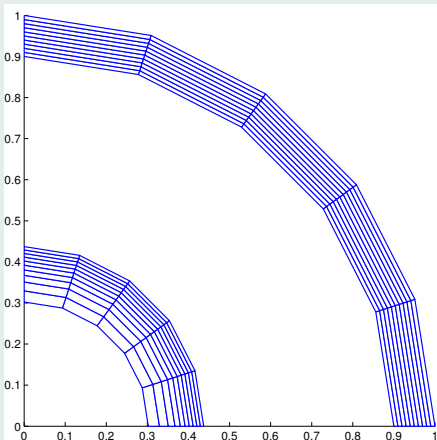
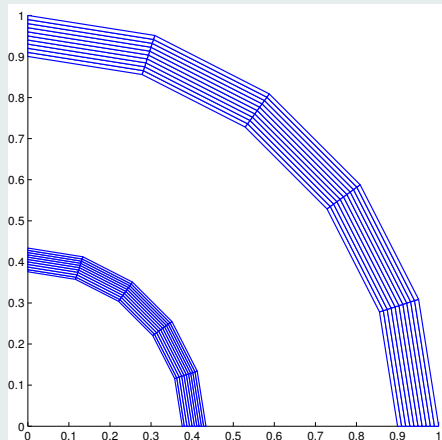


Figure : Density profiles at time  $t = 1$ , on a  $20 \times 18$  polar grid

# Kidder isentropic compression



(g) 1st order



(h) 2nd order

Figure : Initial and final grids for a Kidder problem on a  $10 \times 5$  polar mesh

# Kidder isentropic compression

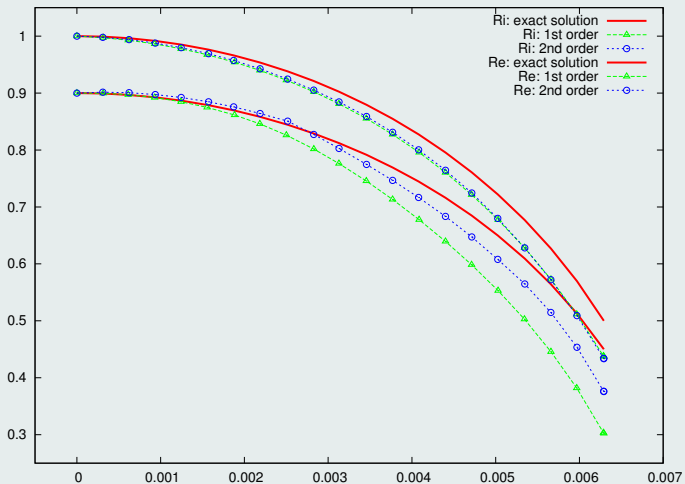
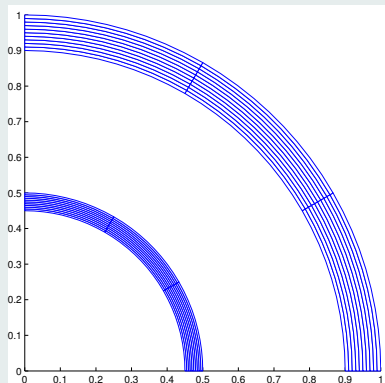
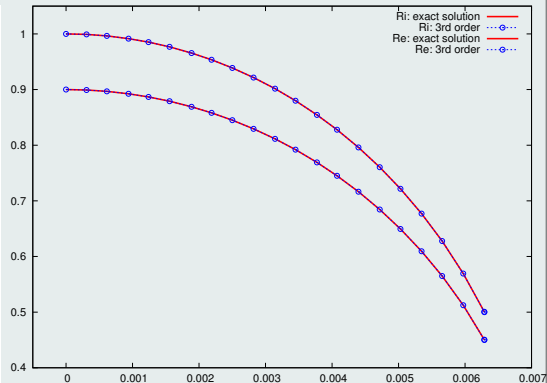


Figure : Interior and exterior shell radii evolution for a Kidder problem on a  $10 \times 5$  polar mesh

# Kidder isentropic compression



(i) Initial and final grids



(j) Shell radii evolution

**Figure :** 3rd order solution for a Kidder compression problem on a  $10 \times 3$  polar grid



# Accuracy and computational time for a Taylor-Green vortex

D.O.F	$N$	$E_{L_1}^h$	$E_{L_2}^h$	$E_{L_\infty}^h$	time (sec)
600	$24 \times 25$	2.67E-2	3.31E-2	8.55E-2	2.01
2400	$48 \times 50$	1.36E-2	1.69E-2	4.37E-2	11.0






Table: 1st order scheme

D.O.F	$N$	$E_{L_1}^h$	$E_{L_2}^h$	$E_{L_\infty}^h$	time (sec)
630	$14 \times 15$	2.76E-3	3.33E-3	1.07E-2	2.77
2436	$28 \times 29$	7.52E-4	9.02E-4	2.73E-3	11.3

Table: 2nd order scheme

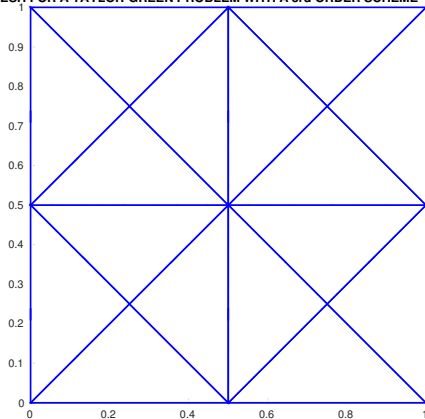
D.O.F	$N$	$E_{L_1}^h$	$E_{L_2}^h$	$E_{L_\infty}^h$	time (sec)
600	$10 \times 10$	2.67E-4	3.36E-4	1.21E-3	4.00
2400	$20 \times 20$	3.43E-5	4.36E-5	1.66E-4	30.6

Table: 3rd order scheme

-  F. VILAR, P.-H. MAIRE AND R. ABGRALL, *Cell-centered discontinuous Galerkin discretizations for two-dimensional scalar conservation laws on unstructured grids and for one-dimensional Lagrangian hydrodynamics*. CAF, 2010.
-  F. VILAR, *Cell-centered discontinuous Galerkin discretization for two-dimensional Lagrangian hydrodynamics*. CAF, 2012.
-  F. VILAR, P.-H. MAIRE AND R. ABGRALL, *A discontinuous Galerkin discretization for solving the two-dimensional gas dynamics equations written under total lagrangian formulation on general unstructured grids*. JCP, 2014.
-  F. VILAR, C.-W. SHU AND P.-H. MAIRE, *Positivity-preserving cell-centered Lagrangian schemes for multi-material compressible flows: Form first-order to high-orders. Part I: The 1D case*. JCP, 2016.
-  F. VILAR, C.-W. SHU AND P.-H. MAIRE, *Positivity-preserving cell-centered Lagrangian schemes for multi-material compressible flows: Form first-order to high-orders. Part II: The 2D case*. JCP, 2016.

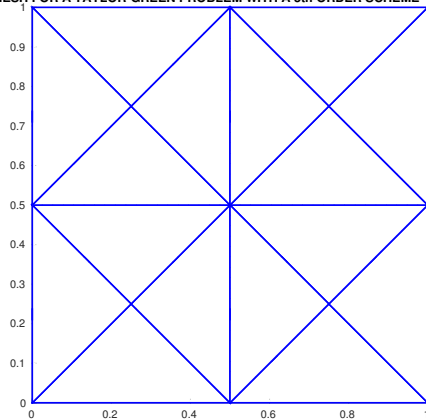
# Taylor-Green vortex

MESH FOR A TAYLOR-GREEN PROBLEM WITH A 3rd ORDER SCHEME



(k) 3rd order

MESH FOR A TAYLOR-GREEN PROBLEM WITH A 5th ORDER SCHEME



(l) 5th order

Figure : Final deformed grids at time  $t = 0.6$ , for 16 triangular cells meshes

# Taylor-Green vortex

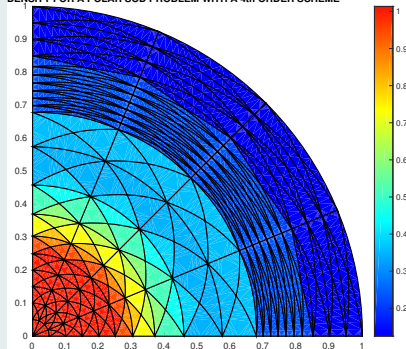
(k) 3rd order

(l) 5th order

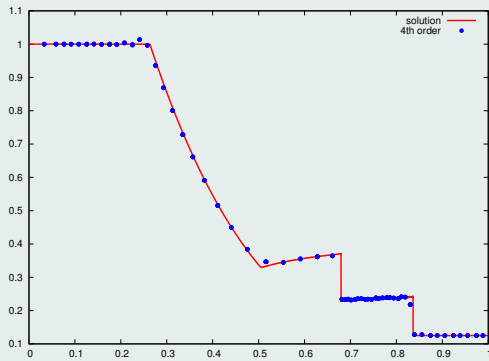
Figure : Final deformed grids at time  $t = 0.6$ , for 16 triangular cells meshes

# Sod shock tube problem - symmetry preservation

DENSITY FOR A POLAR SOD PROBLEM WITH A 4th ORDER SCHEME



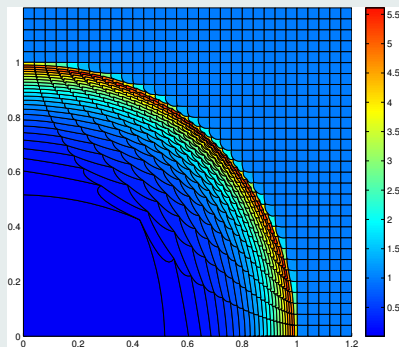
(m) Density field



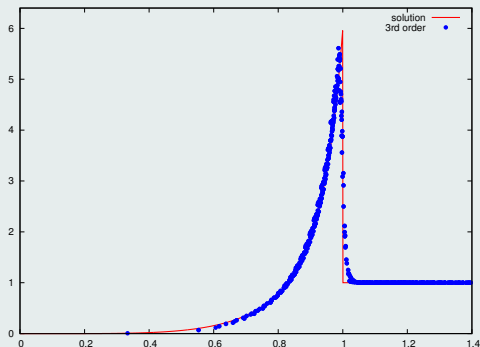
(n) Density profiles

Figure : 4th order solution for a Sod shock tube problem on a polar grid made of 308 triangular cells

# Sedov point blast problem - spurious deformations



(o) Density field



(p) Density profiles

**Figure :** Third-order solution at time  $t = 1$  for a Sedov problem on a  $30 \times 30$  Cartesian mesh